Report

Current Biology

Unlocking crowding by ensemble statistics

Highlights

- Crowding cannot be explained by local feature interactions
- Crowding depends on ensemble statistics
- Crowding strength can be estimated by the parameters of the flanker's distribution

Authors

Natalia A. Tiurina, Yuri A. Markov, Oh-Hyeon Choung, Michael H. Herzog, David Pascucci

Correspondence

nataliatiurina@gmail.com

In brief

In crowding, flankers deteriorate the perception of a target. Crowding depends on the spatial layout of the entire stimulus configuration. However, the number of potential configurations is virtually infinite. Tiurina et al. show that the (orientation) distribution of the flanker configuration is sufficient to determine crowding strength.

Tiurina et al., 2022, Current Biology *32*, 4975–4981
November 21, 2022
https://doi.org/10.1016/j.cub.2022.10.003

CellPress

Current Biology

CellPress

Report

Unlocking crowding by ensemble statistics

Natalia A. Tiurina,[1,2,3,*] Yuri A. Markov,[1] Oh-Hyeon Choung,[1] Michael H. Herzog,[1] and David Pascucci[1]
[1]Laboratory of Psychophysics, Brain Mind Institute, École Polytechnique Fédérale de Lausanne (EPFL), Lausanne CH-1015, Switzerland
[2]Twitter: @na_tiurina
[3]Lead contact
*Correspondence: nataliatiurina@gmail.com
https://doi.org/10.1016/j.cub.2022.10.003

SUMMARY

In crowding,[1–7] objects that can be easily recognized in isolation appear jumbled when surrounded by other elements.[8] Traditionally, crowding is explained by local pooling mechanisms,[3,6,9–15] but many findings have shown that the global configuration of the entire stimulus display, rather than local aspects, determines crowding.[8,16–28] However, understanding global configurations is challenging because even slight changes can lead from crowding to uncrowding and vice versa.[23,25,28,29] Unfortunately, the number of configurations to explore is virtually infinite. Here, we show that one does not need to know the specific configuration of flankers to determine crowding strength but only their ensemble statistics, which allow for the rapid computation of groups within the stimulus display.[30–37] To investigate the role of ensemble statistics in (un)crowding, we used a classic vernier offset discrimination task in which the vernier was flanked by multiple squares. We manipulated the orientation statistics of the squares based on the following rationale: a central square with an orientation different from the mean orientation of the other squares stands out from the rest and groups with the vernier, causing strong crowding. If, on the other hand, all squares group together, the vernier is the only element that stands out, and crowding is weak. These effects should depend exclusively on the perceived ensemble statistics, i.e., on the mean orientation of the squares and not on their individual orientations. In two experiments, we confirmed these predictions.

RESULTS

Experiment 1A

Observers discriminated the offset of a vernier presented alone (vernier alone), surrounded by one square (single square) or by 35 squares (Figures 1 and 2). In one of the conditions with 35 squares, all the squares had an orientation of 0° (identical squares). In the other conditions, we kept the orientation of the central square at 0° and manipulated the orientation distribution of the other 34 squares.

We varied two parameters of the distribution: mean and shape. The mean was equal to 0° in the condition referred to as "mean" because the orientation of the central square corresponded to the mean of all the squares (i.e., 0°). In the "shifted" condition, the mean of the distribution was ±26° because the mean of the 34 squares was shifted clockwise or counterclockwise by 26° relative to the 0° orientation of the central square (Figure 2; method details). The shape of the distribution was "narrow" with a standard deviation (σ) of 3°, "wide" (σ = 10°), or "two peak" (two narrow distributions with peaks separated by 16°). Additionally, we tested a "uniform" distribution in the range from −45° to +45° around the mean (see method details).

A two-way repeated-measures ANOVA showed that vernier thresholds were affected by the type of distribution ($F(2,26)$ = 5.854, p = 0.008, and η^2 = 0.066) and by the difference between the orientation of the central square and the mean orientation of the other squares ($F(1,11)$ = 19.547, p < 0.001, and η^2 = 0.306; interaction, $F(2,26)$ = 3.001, p = 0.067, and η^2 = 0.052). In the "narrow mean" condition, crowding was drastically reduced, compared with the condition without any square (vernier alone; Figure 3A; Table S1). Crowding increased when the orientation of the central square was the mean of a wide and a two-peak distribution (Figure 3A). In these latter two conditions, thresholds were close to typical conditions of strong crowding, such as the single square and uniform (Figure 3A; Table S1). In all conditions where the orientation of the central square was different from the mean of the other squares (e.g., all shifted conditions), crowding was as strong as in the presence of a single square. In the narrow condition, crowding increased linearly as a function of the difference between the central square's orientation and the mean orientation of the other squares (Figure S1).

Experiment 1B

For our rationale, it is important that participants indeed clearly computed the mean of the distributions. Here, we show that this is the case (Figure 3B). We asked the same participants to perform an orientation averaging task on the same displays but without the vernier (method details). In this task, observers reproduced the perceived mean orientation of all 35 squares by rotating a response square with a computer mouse wheel. The errors in the orientation averaging task follow the same pattern as the crowding effects in the mean conditions of the vernier task ($F(3,36)$ = 112.085, p < 0.001, and η^2 = 0.903; Figure 3B; Table S2). That is, observers were more precise in reporting the mean of a narrow compared with a wide and two-peak distribution. This demonstrates that conditions in which the mean

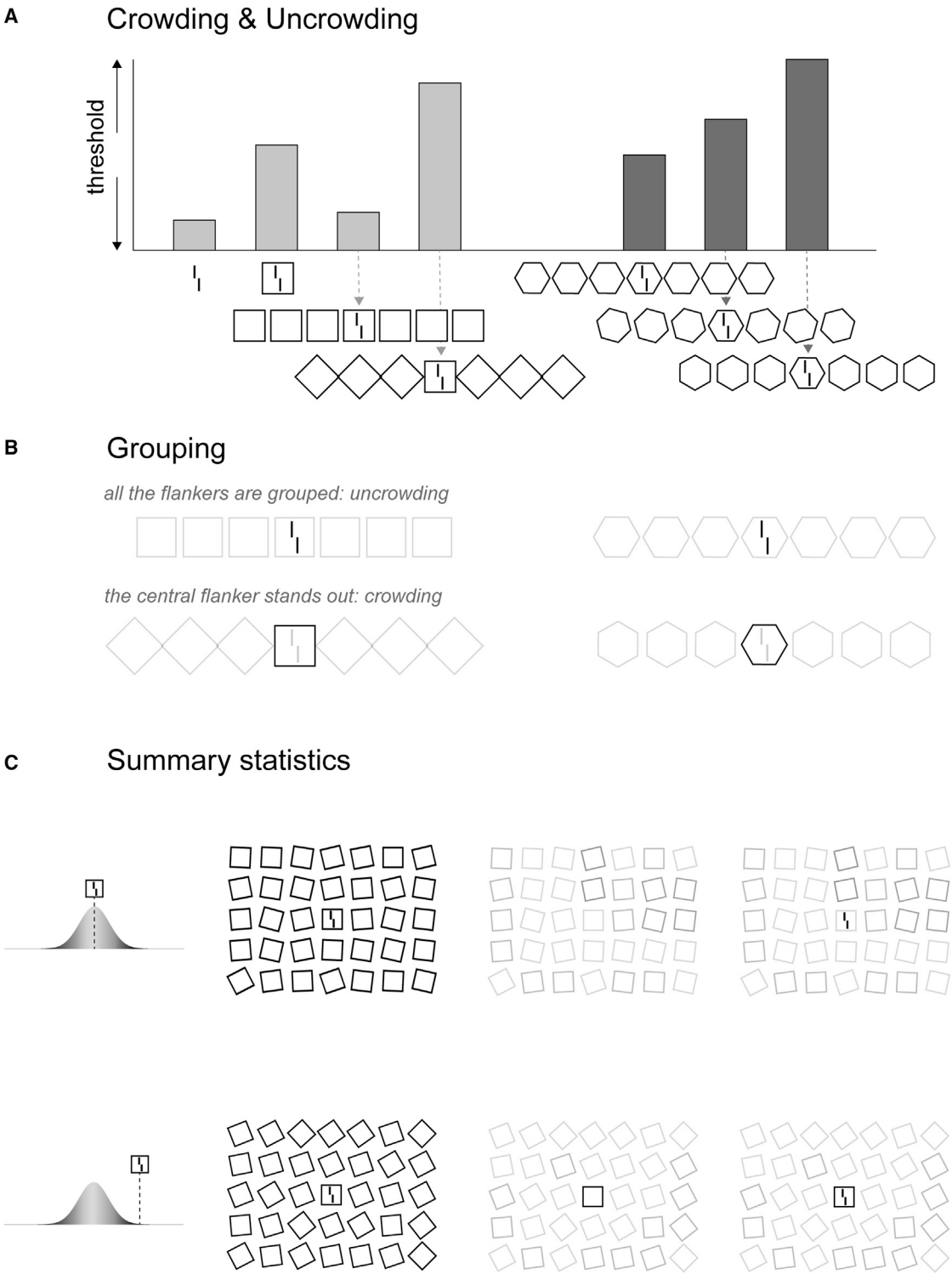

Figure 1. Crowding and uncrowding

(A) Participants reported whether the offset of the lower segment of the vernier was offset to the left or right, compared with the upper segment. Thresholds increase when the vernier is presented within a surrounding square, a typical example of crowding. When six additional squares are presented, crowding is reduced, i.e., uncrowding. These effects are strongly influenced by the global configuration of the flankers: when the other squares are different from the central one (e.g., diamonds), crowding is strong again. Similar results occur with all types of shapes: in a configuration with octagons, even small changes in the

(legend continued on next page)

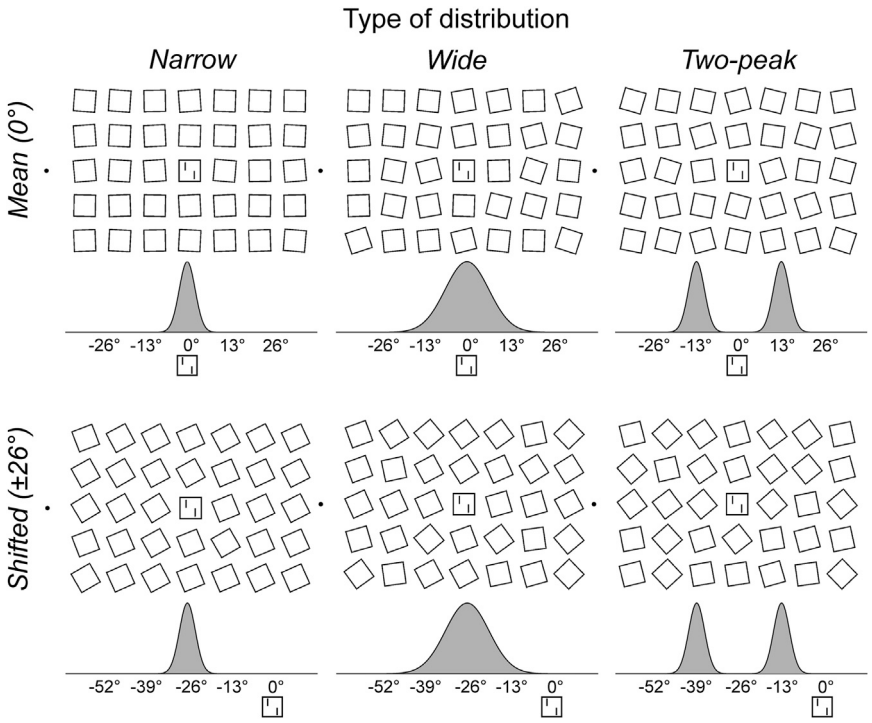

Figure 2. Stimuli and conditions of experiment 1A

The vernier is presented alone, surrounded by one central square or by the central square and 34 other squares. The central square always have a 0° orientation. The orientation of the other squares varies according to three types of distributions (narrow, wide, and two-peak) and whether or not the distribution is shifted. Top row: the orientation of the central square is the same as the mean orientation of all the other squares (0°, mean); bottom row: the orientation of the central square is different from the mean orientation of the other squares because the mean orientation is shifted clockwise or counterclockwise by 26° (shifted). The same displays are used in an orientation averaging task (experiment 1B), except that the vernier is not presented, and the mean orientation of all the squares is randomly determined in each trial. Stimuli are drawn to scale.

orientation can be represented with high precision (e.g., in the narrow condition, experiment 1B) correspond to conditions in which crowding is strongly reduced if the orientation of the central square is equal to the mean of the distribution (narrow mean condition, experiment 1A).

Taken together, our results suggest that the difference between the orientation of the central square and the mean orientation of the other squares determines crowding. In the narrow mean condition, performance is almost as good as in the identical squares condition, indicating that a small orientation jitter still leads to the grouping of the central square with the other squares and uncrowding of the vernier. When the variance of the orientation distribution increases, crowding increases, because we argue that all elements, including the vernier, are grouped. However, it is not the variance itself that determines crowding strength since performance in the ''narrow shifted'' condition is as deteriorated as in the other shifted conditions. We argue that, in particular, in the narrow shifted condition, the central square ungroups from the other squares and groups with the vernier, leading to strong crowding. When the variance increases, all elements, including the vernier, are grouped, and crowding remains strong. Minute details of the stimulus layout and local interactions of and between the entirety of squares do not play any role. It is the overall distribution of the orientation of the squares that matters, i.e., ensemble statistics.

Experiment 2

In experiment 2, the main experiment, we show that crowding is weak when the orientation of the central square is equal to the mean orientation of the other squares—even when none of the orientations of the other squares are similar to the central square orientation (as it is in the narrow mean condition of experiment 1A). We argue that the orientation of the central square fits the ensemble statistics of the orientation distribution of the other squares because its orientation is equal to the mean of the distribution. In experiment 2, we used only the two-peak distribution.

Experiment 2 also addresses a potential confound of experiment 1A. By using different types of distributions, we also changed the probability to have displays in which the central square was directly neighbored by squares of a similar orientation, which is known to reduce crowding.[28] For instance, the decrease in crowding in the narrow mean condition (Figure 3A) could be due to an increase in the probability of highly similar squares near the mean, compared with the wide and two-peak

octagons' orientation can change from crowding to uncrowding and vice versa. The plot schematically depicts findings reported in studies conducted by Manassi et al.[8,28]

(B) Perceptual grouping: when the central square or the central octagon surrounding the vernier groups with the other squares or octagons, the vernier is segmented out from the arrays of the squares and octagons, and crowding decreases (grouped elements are shown in light gray; all stimulus elements are white on a black background). When the central square or octagon does not share the same orientations (dark gray) with the other squares and octagons (light gray), it stands out and groups with the vernier: crowding is strong.

(C) How does the visual system represent groups of multiple elements? A simple strategy is to use ensemble statistics. The upper left panel shows the stimulus display, as shown to the observers, with a central square orientation of 0°. The orientations of the remaining squares are drawn from a distribution with the mean equal to 0° and a small variance (upper left panel). The upper middle panel shows that all squares make up one group (light gray; the vernier is not shown since it is not part of the group). The upper right panel shows that the vernier (black) ungroups from the grouped square array (light gray). Crowding is weak. The lower row shows a situation where the orientation of the other squares is drawn from a distribution with a mean of −26° but with the same variance as in the upper row. The central square stands out from all the other squares (black outline: lower middle panel) and groups with the vernier (lower right panel). Crowding is strong.

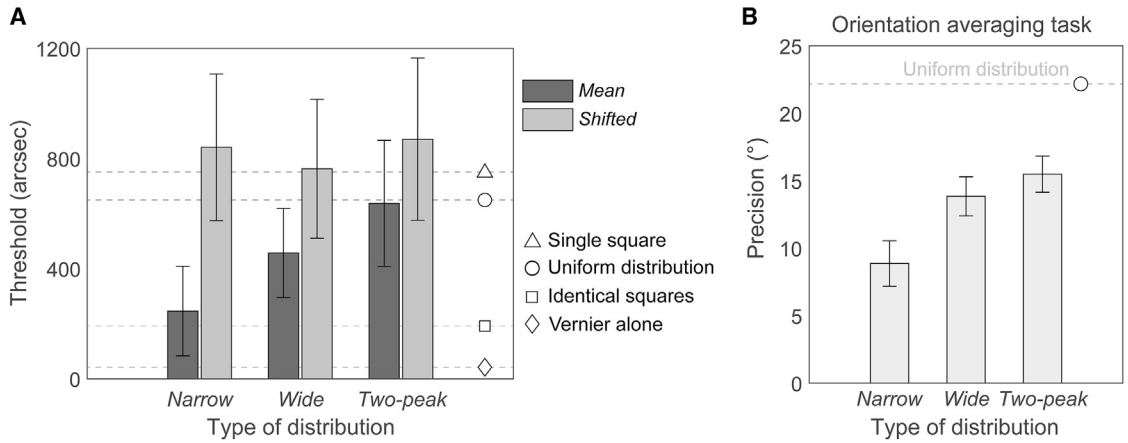

Figure 3. Results of experiment 1

(A) Thresholds for the three types of distributions (narrow, wide, and two-peak) for both the mean (the mean orientation of the distribution is the same as the orientation of the central square; dark gray bars) and shifted conditions (the mean of the distribution is shifted clockwise or counterclockwise by 26°; light gray bars). Single markers and dotted horizontal lines indicate the threshold levels in several reference conditions (method details; supplemental information). We plot performance as thresholds, i.e., high values indicate poor performance and low thresholds indicate good performance.

(B) Results of the orientation averaging task. The results of the averaging task mirror the results of the vernier discrimination task. Error bars denote the 95% t Student confidence interval corrected for repeated measures.[38]

See also Figure S1 and Tables S1 and S2.

distributions. Hence, the results may not be due to the mean orientation but to the difference in orientation between a few squares near the central one.

We shifted the mean orientation of the two-peak distribution, either making the orientation of the central square similar to the mean orientation of all the squares ("grand mean" condition) or similar to the mean of one of the peaks ("at peak" condition). If uncrowding depends on the entire distribution, we should observe uncrowding when the orientation of the central square is the same as the mean orientation of all the squares. Even more, in this latter scenario, crowding should depend on the absolute difference between the orientation of the central square and the mean of the distribution, but not on the local mean of the two peaks. To test this, we included two additional conditions in which the mean of the entire distribution was shifted, and the orientation of the central square could be inside ("shifted inside" condition) or outside of the distribution ("shifted outside" condition; Figure 4; method details). Note that in the shifted inside condition, the orientation of the central square was still close to the mean of the entire distribution, whereas in the shifted outside condition it was far apart. However, in both conditions, the orientation of the central square was equidistant from a local peak.

A one-way repeated-measures ANOVA revealed a significant effect of the difference between the orientation of the central square and the mean orientation of the distribution ($F(3,48)$ = 5.972, p = 0.002, and η^2 = 0.272; Figure 4). As in experiment 1A, crowding increased as the difference in orientation increased (Figure 4; Table S3). Importantly, when the central square's orientation corresponded to the mean of the entire distribution, thresholds were lower than in the at peak condition, where the orientation of the central square was not equal to the mean but was highly similar to the other squares ($t(16)$ = 2.678, p_{holm} = 0.040, and Cohen's d = 0.649). Thresholds were also lower when the orientation of the central square was shifted but remained close to the mean orientation of the other 34 squares (shifted inside), compared with when it was shifted far apart (shifted outside) ($t(16)$ = 2.802, p_{holm} = 0.036, and Cohen's d = 0.601).

DISCUSSION

Here, we demonstrated that a major determinant of crowding is the ensemble statistics of all elements in the display. We showed that in configurations with multiple squares crowding is drastically reduced if the orientation of the central square is equal to the mean orientation of the other squares (experiment 1). This occurred even when none of the orientations in the display was similar to the mean (experiment 2).

Local models cannot explain these findings. For example, a classic explanation is that nearby vertical lines inhibit one another. This might hold for the decrease in crowding in the identical squares condition of experiment 1A, where the vertical lines of nearby squares could inhibit the vertical lines of the central square, eventually uncrowding the vernier. In experiment 2, however, uncrowding occurred when no vertical lines were presented with high probability, except for those of the central square, i.e., local inhibition by similar orientations is impossible (Figure 4, grand mean condition). When the orientation of all the squares was highly similar to the one of the central squares, crowding was stronger (at peak condition). Hence, (un)crowding occurs in a much more abstract space than local interactions and depends on the ensemble statistics of the entire stimulus.

Ensemble statistics must not be confused with image statistics, which is also called summary statistics.[39] For example, in the texture tiling model (TTM), information is pooled over local regions, and a compressed representation of the entire stimulus is created that preserves the statistics of the original image (e.g., mean, variance, 95th percentiles, etc.).[6,13] The degree of

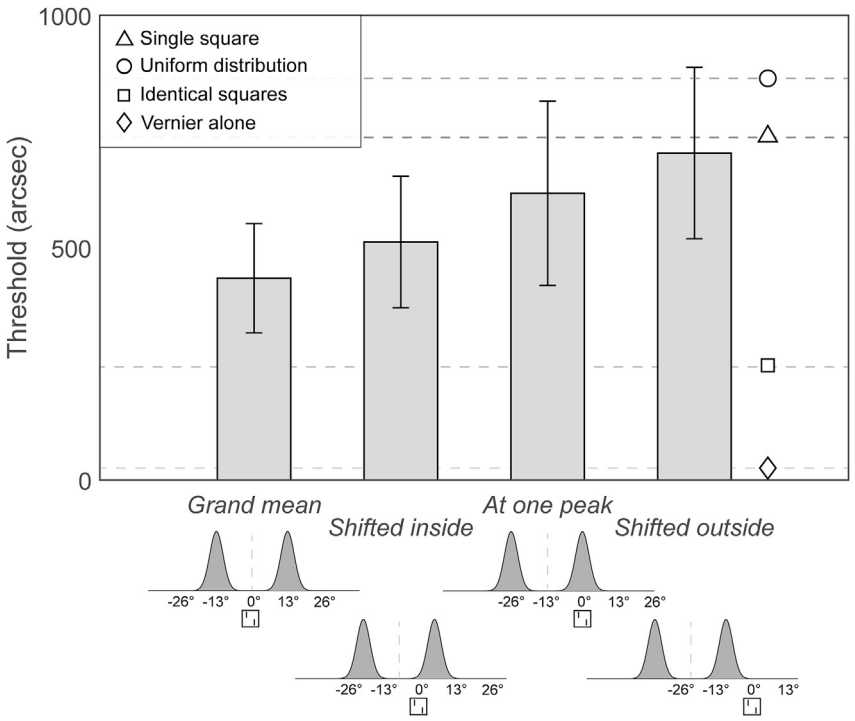

Figure 4. Results of experiment 2

The mean of the whole two-peak distribution is shifted away from the orientation of the central square (fixed at 0°). The y axis shows the corresponding thresholds. Single markers and dotted horizontal lines indicate the threshold level reached in several reference conditions (method details; supplemental information). The gray dashed lines in the legend indicate the means of the distributions. Error bars denote the 95% t Student confidence interval corrected for repeated measures.[38] See also Table S3.

compression determines the strength of crowding. Contrary to image statistics, ensemble statistics are computed over all elements of the display to group elements. Crowding occurs within these groups; TTM may describe crowding within the group. Thus, the only similarity between ensemble statistics and image statistics is that they both use compressed statistical information.

On a neural level, ensemble statistics may involve feedback normalization in which the averaging of local features is followed by normalization via feedback or horizontal connections.[40,41] Normalization has two main consequences: the dampening of local responses to features near the distribution's mean and the enhancement of the response to features that are different from the mean.[40] This mechanism is a prime candidate for the grouping of similar elements[33–36,42] and the segmentation of "outliers," i.e., elements that are different from the statistics of the group.[43,44] Accordingly, a similar mechanism can account for our results: normalization by ensemble statistics may enhance the saliency of a central square, whose orientation is different from the mean orientation in the display, ultimately causing strong crowding of the vernier (Figure 1C).

The effect of ensemble statistics that we found lends key support to a new avenue of models of crowding that emphasize the importance of global processing, incorporating grouping stages.[5] A recent model suggests that the effect of flankers' interference is maximal when the orientation of the target is similar to the average rather than to the individual orientation of the flankers.[45] Similarly, we found that what matters is the mean orientation of all the flankers, but not their individual orientations and local similarities.

Models accounting for global aspects often focus on the relationship between individual elements and their arrangement in space, facing a virtually infinite number of possible configurations.[23,25,28,29,46] Here, we showed that the manipulation of ensemble statistics provides a tool to cope with this issue because ensemble statistics are invariant to the specific spatial arrangement of the elements in the display.

Two major questions have driven research on ensemble statistics in the last decades: (1) whether ensemble statistics are extracted implicitly and in the absence of a task[37,47–51] and (2) what is represented in ensemble statistics (e.g., the mean, variance, or more complex aspects of the distribution).[35,48,52,53] Here, we demonstrated that ensemble statistics are estimated implicitly during a vernier discrimination task that required no judgment of ensemble statistics. This extraction of ensemble statistics had an immediate impact on object recognition (e.g., the vernier discrimination) that depended on the mean orientation of the entire stimulus—but not on more complex aspects, such as the presence of separate local peaks (experiment 2). This suggests that the mean of the entire stimulus is implicitly represented in the absence of an active task about ensemble statistics.[37,48] Notably, the effects of ensemble statistics on crowding were stronger for distributions in which the mean orientation could be estimated with high precision, as tested in a separate explicit task about ensemble statistics (experiment 1B; Figures 3A and 3B). We suggest that ensemble statistics are first built on the entirety of all stimulus elements. The computed ensemble statistics then determine which elements become distorted in crowding and potentially invisible. There is no bottom-up bottleneck in crowding.[54,55] The primary role of ensemble statistics is evident in many other visual phenomena, including visual search.[47,51] Potentially, ensemble statistics may be the primary determinant of vision in general.

STAR★METHODS

Detailed methods are provided in the online version of this paper and include the following:

- KEY RESOURCES TABLE
- RESOURCE AVAILABILITY
  - Lead contact
  - Materials availability
  - Data and code availability

SUPPLEMENTAL INFORMATION

Supplemental information can be found online at https://doi.org/10.1016/j.cub.2022.10.003.

ACKNOWLEDGMENTS

This study was supported by the Swiss Government Excellence Scholarship (ESKAS) awarded by the Federal Commission for Scholarships for Foreign Students (FCS) to N.A.T. and by funding from the Swiss National Science Foundation (grant nos. PZ00P1_179988 and PZ00P1_179988/2) to D.P.; M.H.H. was supported by the Swiss National Science Foundation (SNF) grant 320030_176153 "Basics of visual processing: from elements to figures." The funders had no role in the study design, data collection, and analysis. The authors thank Chris Oriet and an anonymous reviewer for their helpful comments on earlier drafts of the article.

AUTHOR CONTRIBUTIONS

Conceptualization, N.A.T., M.H.H., and D.P.; methodology, N.A.T., Y.A.M., M.H.H., and D.P.; software, N.A.T., Y.A.M., and O.-H.C.; formal analysis, N.A.T., Y.A.M., and O.-H.C.; investigation, N.A.T. and Y.A.M.; writing – original draft, N.A.T., Y.A.M., M.H.H., and D.P.; writing – review & editing, N.A.T., Y.A.M., M.H.H., and D.P.; funding acquisition, N.A.T., M.H.H., and D.P.

DECLARATION OF INTERESTS

The authors declare no competing interests.

Received: August 1, 2022
Revised: August 16, 2022
Accepted: October 3, 2022
Published: October 28, 2022

REFERENCES

1. Bouma, H. (1970). Interaction effects in parafoveal letter recognition. Nature *226*, 177–178.
2. Levi, D.M. (2008). Crowding—an essential bottleneck for object recognition: a mini-review. Vision Res. *48*, 635–654.
3. Pelli, D.G., and Tillman, K.A. (2008). The uncrowded window of object recognition. Nat. Neurosci. *11*, 1129–1135.
4. Whitney, D., and Levi, D.M. (2011). Visual crowding: a fundamental limit on conscious perception and object recognition. Trends Cogn. Sci. *15*, 160–168.
5. Herzog, M.H., Sayim, B., Chicherov, V., and Manassi, M. (2015). Crowding, grouping, and object recognition: a matter of appearance. J. Vis. *15*, 5.
6. Rosenholtz, R., Yu, D., and Keshvari, S. (2019). Challenges to pooling models of crowding: implications for visual mechanisms. J. Vis. *19*, 15.
7. Strasburger, H. (2020). Seven myths on crowding and peripheral vision. iperception. *11*. 2041669520913052.
8. Manassi, M., Sayim, B., and Herzog, M.H. (2013). When crowding of crowding leads to uncrowding. J. Vis. *13*, 10.
9. Parkes, L., Lund, J., Angelucci, A., Solomon, J.A., and Morgan, M. (2001). Compulsory averaging of crowded orientation signals in human vision. Nat. Neurosci. *4*, 739–744.
10. Pelli, D.G., Palomares, M., and Majaj, N.J. (2004). Crowding is unlike ordinary masking: distinguishing feature integration from detection. J. Vis. *4*, 1136–1169.
11. Solomon, J.A., Felisberti, F.M., and Morgan, M.J. (2004). Crowding and the tilt illusion: toward a unified account. J. Vis. *4*, 500–508.
12. Greenwood, J.A., Bex, P.J., and Dakin, S.C. (2009). Positional averaging explains crowding with letter-like stimuli. Proc. Natl. Acad. Sci. USA *106*, 13130–13135.
13. Balas, B., Nakano, L., and Rosenholtz, R. (2009). A summary-statistic representation in peripheral vision explains visual crowding. J. Vis. *9*, 13.1–1318.
14. Rosenholtz, R., Huang, J., Raj, A., Balas, B.J., and Ilie, L. (2012). A summary statistic representation in peripheral vision explains visual search. J. Vis. *12*, 14.
15. Greenwood, J.A., Szinte, M., Sayim, B., and Cavanagh, P. (2017). Variations in crowding, saccadic precision, and spatial localization reveal the shared topology of spatial vision. Proc. Natl. Acad. Sci. USA *114*, E3573–E3582.
16. Põder, E. (2006). Crowding, feature integration, and two kinds of "attention". J. Vis. *6*, 163–169.
17. Malania, M., Herzog, M.H., and Westheimer, G. (2007). Grouping of contextual elements that affect vernier thresholds. J. Vis. *7*, 1–7.
18. Livne, T., and Sagi, D. (2010). How do flankers' relations affect crowding? J. Vis. *10*, 1–14.
19. Livne, T., and Sagi, D. (2007). Configuration influence on crowding. J. Vis. *7*, 4.1–412.
20. Saarela, T.P., Westheimer, G., and Herzog, M.H. (2010). The effect of spacing regularity on visual crowding. J. Vis. *10*, 17.
21. Sayim, B., Westheimer, G., and Herzog, M.H. (2010). Gestalt factors modulate basic spatial vision. Psychol. Sci. *21*, 641–644.
22. Chakravarthi, R., and Pelli, D.G. (2011). The same binding in contour integration and crowding. J. Vis. *11*, 1–12.
23. Doerig, A., Bornet, A., Rosenholtz, R., Francis, G., Clarke, A.M., and Herzog, M.H. (2019). Beyond Bouma's window: how to explain global aspects of crowding? PLoS Comput. Biol. *15*, e1006580.
24. Põder, E. (2020). Crowding and attention in a framework of neural network model. J. Vis. *20*, 19.
25. Bornet, A., Doerig, A., Herzog, M.H., Francis, G., and Van der Burg, E. (2021). Shrinking Bouma's window: how to model crowding in dense displays. PLoS Comput. Biol. *17*, e1009187.
26. Manassi, M., Sayim, B., and Herzog, M.H. (2012). Grouping, pooling, and when bigger is better in visual crowding. J. Vis. *12*, 13.
27. Manassi, M., Hermens, F., Francis, G., and Herzog, M.H. (2015). Release of crowding by pattern completion. J. Vis. *15*, 16.
28. Manassi, M., Lonchampt, S., Clarke, A., and Herzog, M.H. (2016). What crowding can tell us about object representations. J. Vis. *16*, 35.
29. Doerig, A., Bornet, A., Choung, O.H., and Herzog, M.H. (2020). Crowding reveals fundamental differences in local vs. global processing in humans and machines. Vision Res. *167*, 39–45.
30. Ariely, D. (2001). Seeing sets: representation by statistical properties. Psychol. Sci. *12*, 157–162.
31. Alvarez, G.A. (2011). Representing multiple objects as an ensemble enhances visual cognition. Trends Cogn. Sci. *15*, 122–131.
32. Whitney, D., and Yamanashi Leib, A. (2018). Ensemble perception. Annu. Rev. Psychol. *69*, 105–129.
33. Utochkin, I.S. (2015). Ensemble summary statistics as a basis for rapid visual categorization. J. Vis. *15*, 8.
34. Khayat, N., and Hochstein, S. (2019). Relating categorization to set summary statistics perception. Atten. Percept. Psychophys. *81*, 2850–2872.
35. Im, H.Y., Tiurina, N.A., and Utochkin, I.S. (2021). An explicit investigation of the roles that feature distributions play in rapid visual categorization. Atten. Percept. Psychophys. *83*, 1050–1069.

36. Khvostov, V.A., Lukashevich, A.O., and Utochkin, I.S. (2021). Spatially intermixed objects of different categories are parsed automatically. Sci. Rep. *11*, 377.
37. Pascucci, D., Ceylan, G., and Kristjánsson, Á. (2022). Feature distribution learning by passive exposure. Cognition *227*, 105211.
38. Morey, R.D. (2008). Confidence intervals from normalized data: a correction to Cousineau (2005). Tutor. Quant. Methods Psychol. *4*, 61–64.
39. Rosenholtz, R. (2020). Demystifying visual awareness: peripheral encoding plus limited decision complexity resolve the paradox of rich visual experience and curious perceptual failures. Atten. Percept. Psychophys. *82*, 901–925.
40. Haberman, J., and Whitney, D. (2011). Ensemble Perception – Summarizing the Scene and Broadening the Limits of Visual Processing (Haberman & Whitney), pp. 339–349.
41. Utochkin, I.S., Choi, J., and Chong, S.C. (2022). A population response model of ensemble coding. Preprint at bioRxiv. https://doi.org/10.1101/2022.01.19.476871.
42. Utochkin, I.S., Khvostov, V.A., and Stakina, Y.M. (2018). Continuous to discrete: ensemble-based segmentation in the perception of multiple feature conjunctions. Cognition *179*, 178–191.
43. Haberman, J., and Whitney, D. (2010). The visual system discounts emotional deviants when extracting average expression. Atten. Percept. Psychophys. *72*, 1825–1838.
44. Epstein, M., Quilty-Dunn, J., Mandelbaum, E., and Emmanouil, T.A. (2020). The outlier paradox: the role of iterative ensemble coding in discounting outliers. J. Exp. Psychol. Hum. Percept. Perform. *46*, 1267–1279.
45. Cicchini, G.M., D'Errico, G., and Burr, D. (2022). Crowding results from optimal integration of visual targets with contextual information. Nat.Commun. *13*, 5741.
46. Choung, O.H., Bornet, A., Doerig, A., and Herzog, M.H. (2021). Dissecting (un)crowding. J. Vis. *21*, 10.
47. Chetverikov, A., Campana, G., and Kristjánsson, Á. (2016). Building ensemble representations: how the shape of preceding distractor distributions affects visual search. Cognition *153*, 196–210.
48. Chetverikov, A., Campana, G., and Kristjánsson, Á. (2017). Rapid learning of visual ensembles. J. Vis. *17*, 21.
49. Chetverikov, A., Hansmann-Roth, S., Tanrıkulu, Ö.D., and Kristjánsson, Á. (2019). Feature distribution learning (FDL): a new method for studying visual ensembles perception with priming of attention shifts. Neuromethods *151*, 37–57.
50. Hansmann-Roth, S., Kristjánsson, Á., Whitney, D., and Chetverikov, A. (2021). Dissociating implicit and explicit ensemble representations reveals the limits of visual perception and the richness of behavior. Sci. Rep. *11*, 3899.
51. Corbett, J.E., and Melcher, D. (2014). Stable statistical representations facilitate visual search. J. Exp. Psychol. Hum. Percept. Perform. *40*, 1915–1925.
52. Atchley, P., and Andersen, G.J. (1995). Discrimination of speed distributions: sensitivity to statistical properties. Vision Res. *35*, 3131–3144.
53. Dakin, S.C., and Watt, R.J. (1997). The computation of orientation statistics from visual texture. Vision Res. *37*, 3181–3192.
54. Manassi, M., and Whitney, D. (2018). Multi-level crowding and the paradox of object recognition in clutter. Curr. Biol. *28*, R127–R133.
55. Herzog, M.H., and Manassi, M. (2015). Uncorking the bottleneck of crowding: a fresh look at object recognition. Curr. Opin. Behav. Sci. *1*, 86–93.
56. Brainard, D.H. (1997). The psychophysics toolbox. Spat. Vis. *10*, 433–436.
57. Pelli, D.G. (1997). The VideoToolbox software for visual psychophysics: transforming numbers into movies. Spat. Vis. *10*, 437–442.
58. Fründ, I., Haenel, N.V., and Wichmann, F.A. (2011). Inference for psychometric functions in the presence of nonstationary behavior. J. Vis. *11*, 1–19.
59. JASP Team. (2022). JASP (Version 0.16.0). https://jasp-stats.org.
60. Bach, M. (1996). The Freiburg visual acuity test - automatic measurement of visual acuity. Optom. Vis. Sci. *73*, 49–53.
61. Saarela, T.P., Sayim, B., Westheimer, G., and Herzog, M.H. (2009). Global stimulus configuration modulates crowding. J. Vis. *9*, 5.1–511.
62. World Medical Association (2013). World Medical Association Declaration of Helsinki: ethical principles for medical research involving human subjects. JAMA *310*, 2191–2194.
63. Im, H.Y., and Halberda, J. (2013). The effects of sampling and internal noise on the representation of ensemble average size. Atten. Percept. Psychophys. *75*, 278–286.
64. Utochkin, I.S., and Tiurina, N.A. (2014). Parallel averaging of size is possible but range-limited: a reply to Marchant, Simons, and De Fockert. Acta Psychol., *146* (Amst), pp. 7–18.
65. Maule, J., and Franklin, A. (2015). Effects of ensemble complexity and perceptual similarity on rapid averaging of hue. J. Vis. *15*, 6.
66. Taylor, M.M., and Creelman, C.D. (1967). PEST: efficient estimates on probability functions. J. Acoust. Soc. Am. *41*, 782–787.

STAR★METHODS

KEY RESOURCES TABLE

REAGENT or RESOURCE	SOURCE	IDENTIFIER
Deposited data		
Experimental data	Zenodo	[https://doi.org/10.5281/zenodo.7085772]
Experimental models: Organisms/strains		
44 participants in total (19 in experiment 1, 8 females, M_{age} = 23.84 years, SD = 3.88; 25 in experiment 2, 6 females, M age = 22.32 years, SD = 3.2)	N/A	N/A
Software and algorithms		
MATLAB, R2015a	Mathworks	https://matlab.mathworks.com
PsychToolbox	Brainard et al.[56]	http://psychtoolbox.org/download
VideoToolbox	Pelli[57]	N/A
Psignifit 2.5 toolbox	Fründ et al.[58]	http://psignifit.sourceforge.net
JASP	JASP Team[59]	https://jasp-stats.org

RESOURCE AVAILABILITY

Lead contact

Further information and requests for resources should be directed to and will be fulfilled by the lead contact, Natalia Tiurina (nataliatiurina@gmail.com).

Materials availability

No materials are available for this study.

Data and code availability

- The data generated during this study are available at Zenodo: https://doi.org/10.5281/zenodo.7085772
- This paper does not report original code.
- Any additional information required to reanalyze the data reported in this paper is available from the lead contact upon request.

EXPERIMENTAL MODEL AND SUBJECT DETAILS

A total of 44 participants (19 in experiment 1, 8 females, M_{age} = 23.84 years, SD = 3.88; 25 in experiment 2, 6 females, M age = 22.32 years, SD = 3.2), mostly students and staff members of the École Polytechnique Fédérale de Lausanne (EPFL) and the University of Lausanne (UNIL), participated in the experiment for monetary compensation (20 CHF per hour). All participants had normal or corrected-to-normal vision, with acuity values of or above 1.0 determined with both eyes open (Freiburg Visual Acuity Test).[60]

The sample size was determined based on previous studies with similar paradigms.[8,26,28,61] Five participants were excluded in experiment 1 and eight in experiment 2 due to floor performance (high thresholds) in the experimental conditions.

All experiments were conducted following the Declaration of Helsinki[62] except for preregistration and were approved by the local ethics committee.

METHOD DETAILS

Apparatus and stimuli

The stimuli were presented at a viewing distance of 75 cm on an Asus VG248QE LCD monitor (1920x1080 pixels, 120Hz, 24.0") using Matlab (R2015a, 64 bits) and the Psychophysics toolbox.[56,57] Participants used a Logitech RX250 computer mouse (operating resolution: 1000 dpi) and two hand-held push buttons to respond.

The stimuli were white (100 cd/m^2) on a black background with a luminance below 0.3 cd/m^2. Participants were asked to fixate on a red fixation dot (diameter of 8 arcmin, 20 cd/m^2). The target was a vernier comprising two white vertical lines, 30 arcmin long, 1.8 arcmin wide, and separated by a vertical gap of 3 arcmin. Anti-aliasing was used to draw the lines. The offset of the vernier was between 0.17 arcmin and 33.32 arcmin. Following previous studies,[28] the vernier was positioned at 9° to the right from the fixation point. The flankers were all squares (size: 84 x 84 arcmin, 0°) spaced 12 arcmin apart (the center-to-center distance between flankers was 130.8 arcmin).

Experiment 1 consisted of two separate tasks performed by the same participants: the vernier offset discrimination task (experiment 1A) and the orientation averaging task (experiment 1B). In the vernier task, we manipulated the number and orientation of the squares. Four conditions served as a general reference for performance under crowding and uncrowding. In the *Vernier alone* condition, only the target vernier was presented (e.g., no crowding). In the *Identical squares* condition, all squares had the same orientation (0°) as in typical uncrowding displays.[28] In the *Single square* condition, a single square surrounded the vernier (e.g., crowding). In the *Uniform* condition, the orientation of the 35 squares was drawn from a uniform distribution ranging from -45° to +45° (the minimum difference between orientations (step) = 2.5°).

In another set of displays, we used three probability distributions to determine the orientation of the squares: 1) *Narrow* (single mean; σ = 3°; range = 10° (e.g., in the *Narrow Mean* condition from -5° to 5°); the minimum difference between orientations (step) = 1°; see Figure 2, first column); 2) *Wide* (single mean; σ = 10°; range = 36°; step = 4°; see Figure 2, second column); 3) Two-*peak* (consisted of two narrow distributions with a mean-to-mean separation of 16°, and with the same range as wide distribution; range = 36°; step = 1°; see Figure 2, third column). We used these distribution types because the mean orientation is easier to compute in the *Narrow* compared to the *Wide*, *Two-peak*, and *Uniform* distributions.[63–65]

In all the conditions with vernier and squares, the central square was always up-right, i.e., 0°, and we varied the difference in degrees of the distributions' mean from 0°. In the *Mean* condition, the mean of the orientations' distribution was 0° (corresponding to the orientation of the central square, Figure 2, first line). In the *Shifted* condition, the mean of the orientations' distribution was shifted to ±26° (and ±13° in an additional control condition for *Narrow* distribution, see experiment 1; Figure 2, second line).

In the orientation averaging task (experiment 1B), participants were presented with the same displays used in the *Narrow*, *Wide*, *Two-peak*, and *Uniform* conditions, with the following exceptions: the mean of the distribution was randomly chosen from 0° to 90°; the vernier stimulus was not presented; the orientation of the central square was not fixed at 0° but could vary randomly within the chosen distribution. One participant performed only the vernier offset discrimination task but not the orientation averaging task.

In experiment 2, participants performed a vernier offset discrimination task as in experiment 1, but only under a *Two-peak* distribution of orientations. The orientation of the central square was always equal to 0°. In different conditions, we shifted the mean of the distribution in such a way that the orientation of the central square could be: 1) the same as the overall mean of the entire distribution (*Grand mean* condition); 2) the same as the mean of one of the two peaks and shifted by ±13° from the grand mean (*At peak* condition); 3) shifted from the overall mean by ±6° but inside the whole distribution (*Shifted inside* condition); 4) shifted from the overall mean by ±19° and outside of the whole distribution (*Shifted outside* condition). As in experiment 1, additional conditions included the *Vernier alone*, *Single square*, *Identical squares*, and *Uniform*.

Procedure

The experiments were carried out in a dimly lit room ($\sim$ 0.5 lux). Participants were seated at 75 cm from the monitor and were asked to maintain their gaze on a central fixation point throughout the experiment. The stimuli were shown for 150 ms.

In the vernier discrimination tasks, participants were asked to report the offset (left vs. right) of the lower segment of the vernier compared to the upper segment via two hand-held push buttons within 3 seconds. Auditory feedback followed response errors (brief high-pitched beep) and omissions (brief low-pitched beep), and the omitted trials were repeated in the same block at a random later trial. Before the main experimental conditions, each participant performed the task with 100 *Vernier alone* trials first and then 100 *Single square* trials. The main experimental conditions (9 displays) were tested in a block of 100 trials. To compensate for possible learning or sequential effects, the order of conditions in each block was randomized throughout the experiment and across participants. An adaptive staircase procedure (PEST)[66] was used to determine the vernier offset for which participants reached 75% correct responses for each condition.

In the orientation averaging task, participants were asked to reproduce the perceived mean orientation of the flanking squares by rotating a probe square presented around the fixation point. The orientation of the probe was randomly initiated in each trial. The probe was rotated with a mouse wheel. Participants had to click on the left mouse button to submit their answers.

QUANTIFICATION AND STATISTICAL ANALYSIS

In the analysis of vernier offset discrimination, threshold values for 75% of accuracy were estimated by fitting a cumulative Gaussian function to the data using the Psignifit 2.5 toolbox.[58] To avoid vernier stimuli overlapping with squares, we restricted the PEST procedure to 33.32 arcmins (i.e., twice the starting value of 16.67 arcmins). Threshold data (see data and code availability for access to data) were analyzed with a Repeated Measures ANOVA and Bonferroni-Holm post-hoc tests for pairwise comparisons using JASP 0.16.0.0.[59]

To quantify performance in the orientation averaging task, we estimated a measure of error according to the following formula:

$$Error = M_i(bias)$$

where M_i is the average bias for the i-th participant, and *bias* is computed from the reported and the true average orientation, as $reported - true$.